bioRxiv preprint doi: https://doi.org/10.1101/202937; this version posted October 30, 2017. The copyright holder for this preprint (which was not certified by peer review) is the author/funder. All rights reserved. No reuse allowed without permission.

Genomic Locus Modulating IOP in the BXD RI Mouse Strains

Rebecca King[1], Ying Li[1], Jiaxing Wang[1,2], Felix L. Struebing[1] and Eldon E. Geisert[1]

[1]Department of Ophthalmology, Emory University 1365B Clifton Road NE Atlanta GA, 30322

[2]Department of Ophthalmology, Tianjin Medical University General Hospital, Tianjin, China

Corresponding Author: Eldon E. Geisert
Professor of Ophthalmology
Emory University
1365B Clifton Road NE
Atlanta GA 30322
email: egeiser@emory.edu
Phone: 404-778-4239

bioRxiv preprint doi: https://doi.org/10.1101/202937; this version posted October 30, 2017. The copyright holder for this preprint (which was not certified by peer review) is the author/funder. All rights reserved. No reuse allowed without permission.

Abstract

Purpose: Intraocular pressure (IOP) is the primary risk factor for developing glaucoma. The present study examines genomic contribution to the normal regulation of IOP in the mouse.

Methods: The BXD recombinant inbred (RI) strain set was used to identify genomic loci modulating IOP. We measured the IOP from 532 eyes from 33 different strains. The IOP data will be subjected to conventional quantitative trait analysis using simple and composite interval mapping along with epistatic interactions to define genomic loci modulating normal IOP.

Results: The analysis defined one significant quantitative trait locus (QTL) on Chr.8 (100 to 106 Mb). The significant locus was further examined to define candidate genes that modulate normal IOP. There are only two good candidate genes within the 6 Mb over the peak, *Cdh8* (Cadherin 8) and *Cdh11* (Cadherin 11). Expression analysis on gene expression and immunohistochemistry indicate that *Cdh11* is the best candidate for modulating the normal levels of IOP.

Conclusions: We have examined the genomic regulation of IOP in the BXD RI strain set and found one significant QTL on Chr. 8. Within this QTL that are two potential candidates for modulating IOP with the most likely gene being *Cdh11*.

bioRxiv preprint doi: https://doi.org/10.1101/202937; this version posted October 30, 2017. The copyright holder for this preprint (which was not certified by peer review) is the author/funder. All rights reserved. No reuse allowed without permission.

Introduction

Glaucoma is a diverse set of diseases with heterogeneous phenotypic presentations associated with different risk factors. Untreated, glaucoma leads to permanent damage of axons in the optic nerve and visual field loss. Millions of people worldwide are affected [1, 2] and it is the second leading cause of blindness in the United States [3]. Adult-onset glaucoma is a complex collection of diseases with multiple risk factors and genes with differing magnitudes of effects on the eventual loss of RGCs. The severity of the disease appears to be dependent on the interaction of multiple genes, age, and environmental factors [4]. There are also a number of phenotypic risk factors for POAG including: age, ethnicity, central corneal thickness and axial length[5]. The primary risk factor is an elevated intraocular pressure (IOP) [6]. There are known genetic mutations that affect IOP that result in inherited glaucoma [7, 8]. The prime example is MYOC, a protein secreted by the trabecular meshwork and mutations in this protein cause ER stress which results in a decrease in the function of the trabecular meshwork and an elevation in IOP [9, 10]. We know a considerable amount about the regulation of IOP from the production of aqueous humor to the outflow pathways. IOP is a complex trait affected by different tissues in the eye each of which is regulated by multiple genomic loci. Interestingly, there are very few studies that have identified genomic loci modulating normal IOP.

In the present study, we are using the BXD RI strain set that is particularly suited for the study of genetics and the effects on the severity of glaucoma. This genetic reference panel presently consists of 80 strains [11], and we are now in the unique position of being able to study the eyes of more than 80 strains with shuffled genomes from the two parental strains, C57BL/6J and the DBA/2J. There are over 7,000 break points in our current set of BXD strains. For this study, our group has measured IOP of 532 eyes from 33 strains to identify genomic loci modulating IOP. A systems genetics approach to glaucoma is a relatively new branch of quantitative genetics that has the goal of understanding networks of interactions across multiple levels that link DNA variation to phenotype [12]. Systems genetics involves an analysis of sets of causal interactions among classic traits such as IOP, networks of gene variants, and developmental, environmental, and epigenetic factors. The main challenge is the need for comparatively

bioRxiv preprint doi: https://doi.org/10.1101/202937; this version posted October 30, 2017. The copyright holder for this preprint (which was not certified by peer review) is the author/funder. All rights reserved. No reuse allowed without permission.

large sample size and the use of more advanced statistical and computational methods and models. We finally have a sufficiently large number of strains to use this approach [13, 14]. Our goal is now to combine data across several levels from DNA to ocular phenotype and analyze them with newly developed computational methods to understand pre-disease susceptibility to glaucoma along with the genetic networks modulating the response of the eye to elevated IOP.

Methods

Mice: This study measured the IOP in the 33 BXD strains of mice along with the parental strains the C57BL/6J mouse strain and the DBA/2J mouse strain. None of the BXD strains included in this study carried both mutations (*Tyrp1* and *Gpnmb*) known to cause the severe glaucoma phenotype observed in the DBA2/J strain. All of the mice in this study were between 60 and 120 days of age, a time before there is any significant elevation in IOP due pigment dispersion [15]. The data presented in this paper is based on measurements from 532 eyes with roughly equal numbers of male and female mice. All breeding stock was ordered from Jackson Laboratories (Bar Harbor, ME) and maintained at Emory. Mice were housed in the animal facility at Emory University, maintained on a 12 hr light/dark cycle (lights on at 0700), and provided with food and water ad libitum. IOP measurement were made between 0900 and 1100. Both eyes were measured and the data from each eye was entered into the database. An induction–impact tonometer (Tonolab Colonial Medical Supply) was used to measure the IOP according to manufacturer's instructions and as previously described (Saleh M, Nagaraju M, Porciatti 2007; Nagaraju M, Saleh M, Porciatti V 2009). Mice were anesthetized with Avertin (334 mg/kg) or ketamine/xylazine (100,15mg/kg). Three consecutive IOP readings for each eye were averaged. IOP readings obtained with Tonolab have been shown to be accurate and reproducible in various mouse strains, including DBA/2J (Wang et al., 2005). All measurements were taken approximately 10 minutes after the induction of anesthesia. These IOP measurements were made on mice prior to two different experimental procedures, blast injury to the eye or elevation of IOP by injection of magnetic beads into the anterior chamber. When we compared the IOP of animals anesthetized with Avertin

bioRxiv preprint doi: https://doi.org/10.1101/202937; this version posted October 30, 2017. The copyright holder for this preprint (which was not certified by peer review) is the author/funder. All rights reserved. No reuse allowed without permission.

to those anesthetized with ketamine/xylazine over the entire dataset there was not significant difference between the two groups. We did a similar comparison looking only at the C57BL/6J mice with 11 mice anesthetized with Avertin (mean IOP 10.2, SD 0.15) and 27 mice anesthetized with ketamine/xylazine (mean IOP 11.2, SD 2.9) and there was no statistically significant difference between the two groups using a student *t*-test.

Interval Mapping of IOP Phenotype: The IOP data will be subjected to conventional QTL analysis using simple and composite interval mapping along with epistatic interactions. Genotype was regressed against each trait using the Haley-Knott equations implemented in the WebQTL module of GeneNetwork [16] [17] [18]. Empirical significance thresholds of linkage are determined by permutations [19]. We correlate phenotypes with expression data for whole eye and retina generated [13, 20, 21].

Immunohistochemistry: For immunohistochemical experiments mice were deeply anesthetized with a mixture of 15 mg/kg of xylazine (AnaSed) and 100 mg/kg of ketamine (Ketaset) and perfused through the heart with saline followed by 4% paraformaldehyde in phosphate buffer (pH 7.3). The eye were embedded in paraffin as described by Sun et al., [22]. The eyes were dehydrated in a series of ethanol and xylenes changes for 20 minutes each (50% ETOH, 70% ETOH, 90% ETOH, 95% ETOH, two changes of 100% ETOH, 50% ETOH with 50% xylenes, two changes of 100% xylenes, two changes of paraffin. The eyes were then embedded in paraffin blocks. The eyes were sectioned with a rotary microtome at 10µm and mounted on glass slides. The sections were deparaffinized and rehydrated. The sections were rinsed in PBS, and then placed in blocking buffer containing 2% donkey serum, 0.05% DMSO and 0.05% Triton X-100 for 30 min. The sections were rinsed in PBS, and then placed in blocking buffer containing 2% donkey serum, 0.05% DMSO and 0.05% Triton X-100 for 30 min. The sections were incubated in primary antibodies (1:500) against Cadherin 11 (Thermofisher, Cat. #71-7600, Waltham, MA) overnight at 4°C. After rinsing, the sections were incubated with secondary antibody conjugated to AlexaFluor-488 (donkey anti-rabbit, Jackson Immunoresearch Cat #711-545-152, Westgrove, PA) , (1:1000), for 2 hours at room temperature. The sections were then rinsed 3 times in PBS for 15 minutes each. Then

bioRxiv preprint doi: https://doi.org/10.1101/202937; this version posted October 30, 2017. The copyright holder for this preprint (which was not certified by peer review) is the author/funder. All rights reserved. No reuse allowed without permission.

they were counterstained with TO-PRO-3 iodide was purchased from Invitrogen (T3605, Invitrogen, Eugene OR). The slides were flooded with Fluoromount-G (SouthernBiotech Cat #. 0100-01, Birmingham, AL), and covered with a coverslip. All images were photographed using on Nikon Eclipse TE2000-E (Melville, NY) confocal and images were acquired by Nikon's EZ-C1 Software (Bronze Version, 3.91).

PCR Validation: Reverse transcription-quantitative polymerase chain reaction (RT-qPCR) were used to validate the mRNA expression level of Cdh11 and Cdh8 and Myoc in whole eyes of C57BL/6J mice. Primers were designed for Cdh11, Cdh8 and Myoc using Primer BLAST-NCBI so that predicted PCR products were approximately 150bp. The cycle threshold values were normalized to a mouse housekeeping gene peptidylprolyl isomerase A (Ppia). Sequences of the PCR primers are listed in supplementary Table I. PCR reactions were carried out in 10µl reactions containing 5µl of 2x QuantiTect SYBR Green PCR Master Mix (Qiagen, Cat #204141 Hilden, Germany), 0.5 µl of forward primer (0.5µM), 0.5 µl of reverse primer (0.5 µM), 2µl of template cDNA(10ng) and 2µl of RNA free H_2O. PCR of mouse genes was performed using a program beginning at 95°C for 15 min, followed by 40 cycles of reaction with denaturation at 94°C for 15 sec, annealing at 59°C for 30 sec and extension at 72°C for 30 sec of each cycle.

Results

The overall goal of the present investigation was to determine if specific genomic loci modulate IOP in the BXD RI strains. IOP was measured in 532 eyes form 33 BXD RI strains and the two parental strains C57BL/6J mouse and DBA2/J mouse. To create a mapping file the strain averages and standard errors were calculated (Figure 1). The IOP measured across the 33 strains was 13.2 mmHg and the standard deviation was 1.5 mmHg. The strain with the lowest IOP was DBA2/J, with an average IOP of 10.9 mmHg. The strain with the highest IOP was BXD48 with an average IOP of 17.1 mmHg. The IOP of the parental strains was 11.6 mmHg for the C57BL/6J and 10.9 mmHg for the DBA2/J. This is a substantial amount of genetic transgression across the BXD RI strain

bioRxiv preprint doi: https://doi.org/10.1101/202937; this version posted October 30, 2017. The copyright holder for this preprint (which was not certified by peer review) is the author/funder. All rights reserved. No reuse allowed without permission.

set. This type of phenotypic variability is a clear indication that IOP is in fact a complex trait. These data can also be used to calculate the heritability of IOP. Figure 1 reveals a considerable variability in the IOP from strain to strain and the standard error for each strain is rather small. This type of data suggests that the genetic variability has a greater effect than the environmental variability. These data can be used to calculate the heritability of IOP. To calculate heritability (H^2) is the genetic variance (Vg) of the trait is divided by the sum of genetic variance plus the environmental variance (Vg +Ve). The genetic variance can be estimated by taking the standard deviation of the mean of IOP for each strain (Vg = 1.5 mmHg). The environmental variance can be estimated by taking the mean of the standard deviation across the strain (Ve = 3.3 mmHg). Using the formula for heritability, H^2 = Vg/(Vg + Ve), the calculation of 1.5 mmHg /(1.5 mmHg + 3.3 mmHg) reveals that H^2 = 0.31.6. Thus, IOP is a heritability trait in the BXD RI strain set.

Genome Wide Mapping: Taking the average IOP from 33 strains of mice we performed an unbiased genome wide scan to identify genomic loci (QTLs) that modulate IOP. The genome-wide interval map (Figure 2) identifies on significant peak on Chr. 8. Examining an expanded view of Chr.8, 90 to 120 Mb (Figure 3), the peak of the IOP QTL reaches significance form 100 Mb to 106 Mb. BXD strains with higher IOPs (Figure 3B) tend to have the C57BL/6J allele (red) and strains with lower IOPs tend to have the DBA2/J allele (green). When the distribution of genes within this region is examined (gene track Figure 3A) the significant portion of the QTL peak covers a region of the genome that is a gene desert. Within this region there are only 5 genes: *Arl5a* (ADP-ribosylation factor-like 5a), *Cdh11* (cadherin11), *Cdh8* (cadherin 8), *Gm15679* (predicted gene 15679) and *Rplp0* (ribosomal protein, large, P0). Using the tools available on GeneNetwork (genenetwork.org) we are able to identify potential candidates for modulating IOP in the BXD RI strains. The candidate genes can either be genomic elements with cis-QTLs or they can be genes with nonsynonymous SNPs changing protein sequence. Within this region there are only two putative candidate genes. There are cisQTL for *Cdh11*(exon probes 17512155 and 17512156, build 2016-12-12 GeneNetwork). There are two genes in this region with non-synonymous SNPs, *Cdh11* and *Cdh8*. Thus, there is a single QTL

bioRxiv preprint doi: https://doi.org/10.1101/202937; this version posted October 30, 2017. The copyright holder for this preprint (which was not certified by peer review) is the author/funder. All rights reserved. No reuse allowed without permission.

modulating IOP and this peak lies in a gene desert with only two good candidate genes *Cdh11* and *Cdh8*.

For the initial evaluation of the two candidate genes we examined their expression level in microarray datasets hosted on GeneNetwork: the eye database (Eye M430v2 (Sep08) RMA) and retina database (DoD Retina Normal Affy MoGene 2.0 ST (May15) RMA Gene Level). In the eye dataset, the highest level of expression for a Cdh11 probe set (1450757_at) is 10.8 Log_2, while for *Cdh8* (1422052_at) the highest level of expression is 7.3 Log_2. For this dataset the mean expression of mRNA in the retina is set to 8. Thus, *Cdh11* is expressed at levels higher than the mean and *Cdh8* is expressed at levels below the average expression level. Furthermore, in the whole eye database, there is over an 8-fold increase in expression of *Cdh11* relative to *Cdh8*. In the retina database, *Cdh11* (probe set 17512153) had an expression level of 10.9 and *Cdh8* (probe set 17512121) had an expression level of 9.3, indicating that within the retina proper *Cdh11* is expression is 2-fold higher than *Cdh8*.

To confirm the expression levels of *Cdh11* and *Cdh8* in the eye, we examined the levels of mRNA in the whole eye by RT-qPCR. In 4 biological replicate RNA samples, we examined the levels of *Cdh11, Cdh8* and *Myoc* (a marker of trabecular meshwork cells, [23]). Our PCR analysis confirmed the general findings of the microarray data sets. In the 4 biological samples of whole eye, *Cdh11* was more highly expressed than *Cdh8*. The average of the 4 samples demonstrated a more than 2-fold higher expression of *Cdh11* than *Cdh8*. *Myoc* was also expressed at a higher level than *Cdh8* but at approximately at the same level as *Cdh11*. All of these data taken together indicate that *Cdh11* is the prime candidate for an upstream modulator of IOP.

Distribution of Cadherin 11 in the Eye: To determine if cadherin 11 is found in structures associated with the control of IOP, we stained sections of the eye for cadherin 11. In these sections, there was a considerable amount of antibody-specific staining (Fig. 4A). This label is not observed in control sections stained with secondary antibody only (Fig. 4B). There is extensive labeling of all layers of the cornea. The epithelium of the

bioRxiv preprint doi: https://doi.org/10.1101/202937; this version posted October 30, 2017. The copyright holder for this preprint (which was not certified by peer review) is the author/funder. All rights reserved. No reuse allowed without permission.

ciliary body is also heavily labeled as well as labeling of pars plana. There is also light labeling of the retina. At higher magnification (Fig. 4C), clear labeling of the trabecular meshwork (arrow). Thus, cadherin 11 is expressed in the cells of the trabecular meshwork, the primary structure involved in regulating IOP.

Discussion

The normal regulation of intraocular pressure is a balance between production in the ciliary body and outflow [24, 25]. In the human, IOP ranges can range from a relatively low pressures to extremely high that occur in acute angle closure glaucoma. It is generally accepted that the "normal" range for IOP in humans is from 12mmHg to 22mmHg [26, 27]. In addition, monitoring throughout the day reveals IOP is pulsatory and has a diurnal variability [28]. These findings tell an interesting story about the regulation of pressure in the eye; however, the primary driving force behind the intense investigation of IOP in humans is that fact that it is the primary risk factor for developing glaucoma [29]. Furthermore, all of the current treatments for glaucoma center around lowering IOP either by pharmacological approaches or surgery [30, 31].

The association of elevated IOP and glaucoma, has driven most of the study of IOP in human populations [5, 32, 33]. Most of these studies involve the study of glaucoma, but a few have a primary focused on the regulation of IOP. These studies have found that IOP is a heritable trait with estimates of heritability ranging from 0.39 to 0.64 [6, 34-36]. In the present study, we found that the heritability of IOP in the BXD RI strains was 0.36. Thus, the mouse strains demonstrated a heritability near the lower end of the human populations. The interest has prompted studies to identify genes regulating IOP. In a genome-wide association study of IOP involving 11,972 subjects, significant associations were observed with SNPs in two genes, *GAS7* and *TMCO1* [37]. Both of these genes are expressed at high levels in the ciliary body and trabecular meshwork [38] and both of the genes interact with known glaucoma risk genes [37]. TMCO1 is also known to be associated with sever glaucoma risk [39].

bioRxiv preprint doi: https://doi.org/10.1101/202937; this version posted October 30, 2017. The copyright holder for this preprint (which was not certified by peer review) is the author/funder. All rights reserved. No reuse allowed without permission.

In an effort to understand the regulation of IOP and its effects on the retina, many research groups have used inbred mouse strains [40-44]. IOP varies widely across different strains of mice [40, 45], ranging from a low of 11mmHg in the BALB/c mouse strain to a high of 19mmHg in the CBA/Ca mouse strain. In the present study, the average measured IOP across the 33 strains was 13.2mmHg. The lowest measured IOP was 10.9mmHg in the DBA/2J strain and the highest was 17.1mmHg in the BXD48 strain. Using the variability across the BXD RI strains we were able to map a single significant QTL on Chr. 8 in the mouse. The peak of the QTL was in a gene desert and within this region there were only two potential candidate genes that could be modulating IOP in the BXD strain set. Based on expression of mRNA in the eye microarray dataset and the findings of real time PCR *Cdh11* appears to be the best candidate. *Cdh11* is expressed approximately 8-fold higher in the eye than is *Cdh8*. Furthermore, previous study [46] found *CDH11* to be highly expressed in cultured human trabecular meshwork cells. We found that Cadherin 11 is expressed in the trabecular meshwork using indirect immunohistochemistry. All of these data suggest that the expression Cadherin 11 in the trabecular meshwork modulates IOP across the BXD RI strain set.

How is it possible that a cadherin can modulate IOP in the mouse eye? IOP is regulated by fluid resistance at the trabecular meshwork and Schlemm's canal [47, 48]. The stiffness of these structures is determined by the extracellular matrix within the trabecular meshwork and Schlemm's canal and the contractile nature of the cells themselves (Zhou et al. 2012) inner wall was considered to be the most important player regulating such resistance [49-51]. The dysregulation or poor organization of extracellular matrix may increase the fluid resistance, leading to an elevation of the IOP. *Cdh11* was recently revealed to be a novel regulator of extracellular matrix synthesis and tissue mechanics[52] , and it is also found to be highly expressed in cultured human trabecular meshwork cells [46]. It is possible that the IOP can be regulated by *Cdh11* and related pathways by altering the extracellular matrix structure of the trabecular meshwork. Future studies about the role of *Cdh11* in the trabecular meshwork may give insights into the mechanism of IOP modulation.

bioRxiv preprint doi: https://doi.org/10.1101/202937; this version posted October 30, 2017. The copyright holder for this preprint (which was not certified by peer review) is the author/funder. All rights reserved. No reuse allowed without permission.

Acknowledgements: We would like to thank the Robert W Williams and his group for providing a wealth of bioinformatic resources on GeneNetwork.org. We thank Chelsey Faircloth for her assistance in immunostaining. This study was supported by an Unrestricted Grand from Research to Prevent Blindness, NEI grant R01EY017841 (E.E.G.), Owens Family Glaucoma Research Fund, P30EY06360 (Emory Vision Core) and DoD CDMRP Grant W81XWH-12-1-0255 from the USA Army Medical Research & Materiel Command and the Telemedicine and Advanced Technology (E.E.G.).

bioRxiv preprint doi: https://doi.org/10.1101/202937; this version posted October 30, 2017. The copyright holder for this preprint (which was not certified by peer review) is the author/funder. All rights reserved. No reuse allowed without permission.

References

1. European Glaucoma Prevention Study G, Miglior S, Pfeiffer N, Torri V, Zeyen T, Cunha-Vaz J, Adamsons I. Predictive factors for open-angle glaucoma among patients with ocular hypertension in the European Glaucoma Prevention Study. Ophthalmology 2007; 114(1):3-9.
2. Leske MC, Heijl A, Hyman L, Bengtsson B, Dong L, Yang Z, Group E. Predictors of long-term progression in the early manifest glaucoma trial. Ophthalmology 2007; 114(11):1965-72.
3. Medeiros FA, Sample PA, Zangwill LM, Bowd C, Aihara M, Weinreb RN. Corneal thickness as a risk factor for visual field loss in patients with preperimetric glaucomatous optic neuropathy. Am J Ophthalmol 2003; 136(5):805-13.
4. Herndon LW, Weizer JS, Stinnett SS. Central corneal thickness as a risk factor for advanced glaucoma damage. Arch Ophthalmol 2004; 122(1):17-21.
5. Gordon MO, Beiser JA, Brandt JD, Heuer DK, Higginbotham EJ, Johnson CA, Keltner JL, Miller JP, Parrish RK, 2nd, Wilson MR, Kass MA. The Ocular Hypertension Treatment Study: baseline factors that predict the onset of primary open-angle glaucoma. Arch Ophthalmol 2002; 120(6):714-20; discussion 829-30.
6. Klein BE, Klein R, Lee KE. Heritability of risk factors for primary open-angle glaucoma: the Beaver Dam Eye Study. Invest Ophthalmol Vis Sci 2004; 45(1):59-62.
7. Stone EM, Fingert JH, Alward WL, Nguyen TD, Polansky JR, Sunden SL, Nishimura D, Clark AF, Nystuen A, Nichols BE, Mackey DA, Ritch R, Kalenak JW, Craven ER, Sheffield VC. Identification of a gene that causes primary open angle glaucoma. Science 1997; 275(5300):668-70.
8. Wiggs JL. Genetic etiologies of glaucoma. Arch Ophthalmol 2007; 125(1):30-7.
9. Joe MK, Sohn S, Hur W, Moon Y, Choi YR, Kee C. Accumulation of mutant myocilins in ER leads to ER stress and potential cytotoxicity in human trabecular meshwork cells. Biochem Biophys Res Commun 2003; 312(3):592-600.
10. Kasetti RB, Phan TN, Millar JC, Zode GS. Expression of Mutant Myocilin Induces Abnormal Intracellular Accumulation of Selected Extracellular Matrix Proteins in the Trabecular Meshwork. Invest Ophthalmol Vis Sci 2016; 57(14):6058-69.
11. Peirce JL, Lu L, Gu J, Silver LM, Williams RW. A new set of BXD recombinant inbred lines from advanced intercross populations in mice. BMC Genet 2004; 5:7.
12. Mozhui K, Ciobanu DC, Schikorski T, Wang X, Lu L, Williams RW. Dissection of a QTL hotspot on mouse distal chromosome 1 that modulates neurobehavioral phenotypes and gene expression. PLoS Genet 2008; 4(11):e1000260.

bioRxiv preprint doi: https://doi.org/10.1101/202937; this version posted October 30, 2017. The copyright holder for this preprint (which was not certified by peer review) is the author/funder. All rights reserved. No reuse allowed without permission.

13. Geisert EE, Lu L, Freeman-Anderson NE, Templeton JP, Nassr M, Wang X, Gu W, Jiao Y, Williams RW. Gene expression in the mouse eye: an online resource for genetics using 103 strains of mice. Mol Vis 2009; 15:1730-63.
14. Freeman NE, Templeton JP, Orr WE, Lu L, Williams RW, Geisert EE. Genetic networks in the mouse retina: growth associated protein 43 and phosphatase tensin homolog network. Mol Vis 2011; 17:1355-72.
15. Anderson MG, Smith RS, Hawes NL, Zabaleta A, Chang B, Wiggs JL, John SW. Mutations in genes encoding melanosomal proteins cause pigmentary glaucoma in DBA/2J mice. Nat Genet 2002; 30(1):81-5.
16. Chesler EJ, Lu L, Shou S, Qu Y, Gu J, Wang J, Hsu HC, Mountz JD, Baldwin NE, Langston MA, Threadgill DW, Manly KF, Williams RW. Complex trait analysis of gene expression uncovers polygenic and pleiotropic networks that modulate nervous system function. Nat Genet 2005; 37(3):233-42.
17. Rosen GD, La Porte NT, Diechtiareff B, Pung CJ, Nissanov J, Gustafson C, Bertrand L, Gefen S, Fan Y, Tretiak OJ, Manly KF, Park MR, Williams AG, Connolly MT, Capra JA, Williams RW. Informatics center for mouse genomics: the dissection of complex traits of the nervous system. Neuroinformatics 2003; 1(4):327-42.
18. Carlborg O, De Koning DJ, Manly KF, Chesler E, Williams RW, Haley CS. Methodological aspects of the genetic dissection of gene expression. Bioinformatics 2005; 21(10):2383-93.
19. Churchill GA, Doerge RW. Empirical threshold values for quantitative trait mapping. Genetics 1994; 138(3):963-71.
20. King R, Lu L, Williams RW, Geisert EE. Transcriptome networks in the mouse retina: An exon level BXD RI database. Mol Vis 2015; 21:1235-51.
21. Templeton JP, Freeman NE, Nickerson JM, Jablonski MM, Rex TS, Williams RW, Geisert EE. Innate immune network in the retina activated by optic nerve crush. Invest Ophthalmol Vis Sci 2013; 54(4):2599-606.
22. Sun N, Shibata B, Hess JF, FitzGerald PG. An alternative means of retaining ocular structure and improving immunoreactivity for light microscopy studies. Mol Vis 2015; 21:428-42.
23. Takahashi H, Noda S, Imamura Y, Nagasawa A, Kubota R, Mashima Y, Kudoh J, Oguchi Y, Shimizu N. Mouse myocilin (Myoc) gene expression in ocular tissues. Biochem Biophys Res Commun 1998; 248(1):104-9.
24. Brubaker RF. Flow of Aqueous-Humor in Humans - the Friedenwald Lecture. Invest Ophth Vis Sci 1991; 32(13):3145-66.
25. Goel M, Picciani RG, Lee RK, Bhattacharya SK. Aqueous humor dynamics: a review. Open Ophthalmol J 2010; 4:52-9.
26. Hollows FC, Graham PA. Intra-ocular pressure, glaucoma, and glaucoma suspects in a defined population. Br J Ophthalmol 1966; 50(10):570-86.
27. Renard E, Palombi K, Gronfier C, Pepin JL, Noel C, Chiquet C, Romanet JP. Twenty-four hour (Nyctohemeral) rhythm of intraocular pressure and ocular perfusion pressure in normal-tension glaucoma. Invest Ophthalmol Vis Sci 2010; 51(2):882-9.

bioRxiv preprint doi: https://doi.org/10.1101/202937; this version posted October 30, 2017. The copyright holder for this preprint (which was not certified by peer review) is the author/funder. All rights reserved. No reuse allowed without permission.

28. Aptel F, Weinreb RN, Chiquet C, Mansouri K. 24-h monitoring devices and nyctohemeral rhythms of intraocular pressure. Prog Retin Eye Res 2016; 55:108-48.
29. Sommer A, Tielsch JM, Katz J, Quigley HA, Gottsch JD, Javitt J, Singh K. Relationship between intraocular pressure and primary open angle glaucoma among white and black Americans. The Baltimore Eye Survey. Arch Ophthalmol 1991; 109(8):1090-5.
30. Cohen LP, Pasquale LR. Clinical characteristics and current treatment of glaucoma. Cold Spring Harb Perspect Med 2014; 4(6).
31. Gedde SJ, Panarelli JF, Banitt MR, Lee RK. Evidenced-based comparison of aqueous shunts. Curr Opin Ophthalmol 2013; 24(2):87-95.
32. Ojha P, Wiggs JL, Pasquale LR. The genetics of intraocular pressure. Semin Ophthalmol 2013; 28(5-6):301-5.
33. Ozel AB, Moroi SE, Reed DM, Nika M, Schmidt CM, Akbari S, Scott K, Rozsa F, Pawar H, Musch DC, Lichter PR, Gaasterland D, Branham K, Gilbert J, Garnai SJ, Chen W, Othman M, Heckenlively J, Swaroop A, Abecasis G, Friedman DS, Zack D, Ashley-Koch A, Ulmer M, Kang JH, Consortium N, Liu Y, Yaspan BL, Haines J, Allingham RR, Hauser MA, Pasquale L, Wiggs J, Richards JE, Li JZ. Genome-wide association study and meta-analysis of intraocular pressure. Hum Genet 2014; 133(1):41-57.
34. Chang TC, Congdon NG, Wojciechowski R, Munoz B, Gilbert D, Chen P, Friedman DS, West SK. Determinants and heritability of intraocular pressure and cup-to-disc ratio in a defined older population. Ophthalmology 2005; 112(7):1186-91.
35. Carbonaro F, Andrew T, Mackey DA, Young TL, Spector TD, Hammond CJ. Repeated measures of intraocular pressure result in higher heritability and greater power in genetic linkage studies. Invest Ophthalmol Vis Sci 2009; 50(11):5115-9.
36. van Koolwijk LM, Despriet DD, van Duijn CM, Pardo Cortes LM, Vingerling JR, Aulchenko YS, Oostra BA, Klaver CC, Lemij HG. Genetic contributions to glaucoma: heritability of intraocular pressure, retinal nerve fiber layer thickness, and optic disc morphology. Invest Ophthalmol Vis Sci 2007; 48(8):3669-76.
37. van Koolwijk LM, Ramdas WD, Ikram MK, Jansonius NM, Pasutto F, Hysi PG, Macgregor S, Janssen SF, Hewitt AW, Viswanathan AC, ten Brink JB, Hosseini SM, Amin N, Despriet DD, Willemse-Assink JJ, Kramer R, Rivadeneira F, Struchalin M, Aulchenko YS, Weisschuh N, Zenkel M, Mardin CY, Gramer E, Welge-Lussen U, Montgomery GW, Carbonaro F, Young TL, Group DER, Bellenguez C, McGuffin P, Foster PJ, Topouzis F, Mitchell P, Wang JJ, Wong TY, Czudowska MA, Hofman A, Uitterlinden AG, Wolfs RC, de Jong PT, Oostra BA, Paterson AD, Wellcome Trust Case Control C, Mackey DA, Bergen AA, Reis A, Hammond CJ, Vingerling JR, Lemij HG, Klaver CC, van Duijn CM. Common genetic determinants of intraocular pressure and primary open-angle glaucoma. PLoS Genet 2012; 8(5):e1002611.
38. Liton PB, Luna C, Challa P, Epstein DL, Gonzalez P. Genome-wide expression profile of human trabecular meshwork cultured cells,

bioRxiv preprint doi: https://doi.org/10.1101/202937; this version posted October 30, 2017. The copyright holder for this preprint (which was not certified by peer review) is the author/funder. All rights reserved. No reuse allowed without permission.

441 nonglaucomatous and primary open angle glaucoma tissue. Mol Vis 2006;
442 12:774-90.
443 39. Burdon KP, Macgregor S, Hewitt AW, Sharma S, Chidlow G, Mills RA,
444 Danoy P, Casson R, Viswanathan AC, Liu JZ, Landers J, Henders AK, Wood J,
445 Souzeau E, Crawford A, Leo P, Wang JJ, Rochtchina E, Nyholt DR, Martin NG,
446 Montgomery GW, Mitchell P, Brown MA, Mackey DA, Craig JE. Genome-wide
447 association study identifies susceptibility loci for open angle glaucoma at TMCO1
448 and CDKN2B-AS1. Nat Genet 2011; 43(6):574-8.
449 40. Savinova OV, Sugiyama F, Martin JE, Tomarev SI, Paigen BJ, Smith RS,
450 John SW. Intraocular pressure in genetically distinct mice: an update and strain
451 survey. BMC Genet 2001; 2:12.
452 41. Struebing FL, Geisert EE. What Animal Models Can Tell Us About
453 Glaucoma. Prog Mol Biol Transl Sci 2015; 134:365-80.
454 42. Sappington RM, Carlson BJ, Crish SD, Calkins DJ. The microbead
455 occlusion model: a paradigm for induced ocular hypertension in rats and mice.
456 Invest Ophthalmol Vis Sci 2010; 51(1):207-16.
457 43. Cone FE, Gelman SE, Son JL, Pease ME, Quigley HA. Differential
458 susceptibility to experimental glaucoma among 3 mouse strains using bead and
459 viscoelastic injection. Exp Eye Res 2010; 91(3):415-24.
460 44. Samsel PA, Kisiswa L, Erichsen JT, Cross SD, Morgan JE. A novel
461 method for the induction of experimental glaucoma using magnetic
462 microspheres. Invest Ophthalmol Vis Sci 2011; 52(3):1671-5.
463 45. Wang WH, Millar JC, Pang IH, Wax MB, Clark AF. Noninvasive
464 measurement of rodent intraocular pressure with a rebound tonometer. Invest
465 Ophthalmol Vis Sci 2005; 46(12):4617-21.
466 46. Paylakhi SH, Yazdani S, April C, Fan JB, Moazzeni H, Ronaghi M, Elahi
467 E. Non-housekeeping genes expressed in human trabecular meshwork cell
468 cultures. Mol Vis 2012; 18:241-54.
469 47. Ethier CR, Kamm RD, Palaszewski BA, Johnson MC, Richardson TM.
470 Calculations of flow resistance in the juxtacanalicular meshwork. Invest
471 Ophthalmol Vis Sci 1986; 27(12):1741-50.
472 48. Brubaker RF. The effect of intraocular pressure on conventional outflow
473 resistance in the enucleated human eye. Invest Ophthalmol 1975; 14(4):286-92.
474 49. Bradley JM, Vranka J, Colvis CM, Conger DM, Alexander JP, Fisk AS,
475 Samples JR, Acott TS. Effect of matrix metalloproteinases activity on outflow in
476 perfused human organ culture. Invest Ophthalmol Vis Sci 1998; 39(13):2649-58.
477 50. Johnson M. 'What controls aqueous humour outflow resistance?'. Exp Eye
478 Res 2006; 82(4):545-57.
479 51. Vranka JA, Kelley MJ, Acott TS, Keller KE. Extracellular matrix in the
480 trabecular meshwork: intraocular pressure regulation and dysregulation in
481 glaucoma. Exp Eye Res 2015; 133:112-25.
482 52. Row S, Liu Y, Alimperti S, Agarwal SK, Andreadis ST. Cadherin-11 is a
483 novel regulator of extracellular matrix synthesis and tissue mechanics. J Cell Sci
484 2016; 129(15):2950-61.
485

bioRxiv preprint doi: https://doi.org/10.1101/202937; this version posted October 30, 2017. The copyright holder for this preprint (which was not certified by peer review) is the author/funder. All rights reserved. No reuse allowed without permission.

Figures

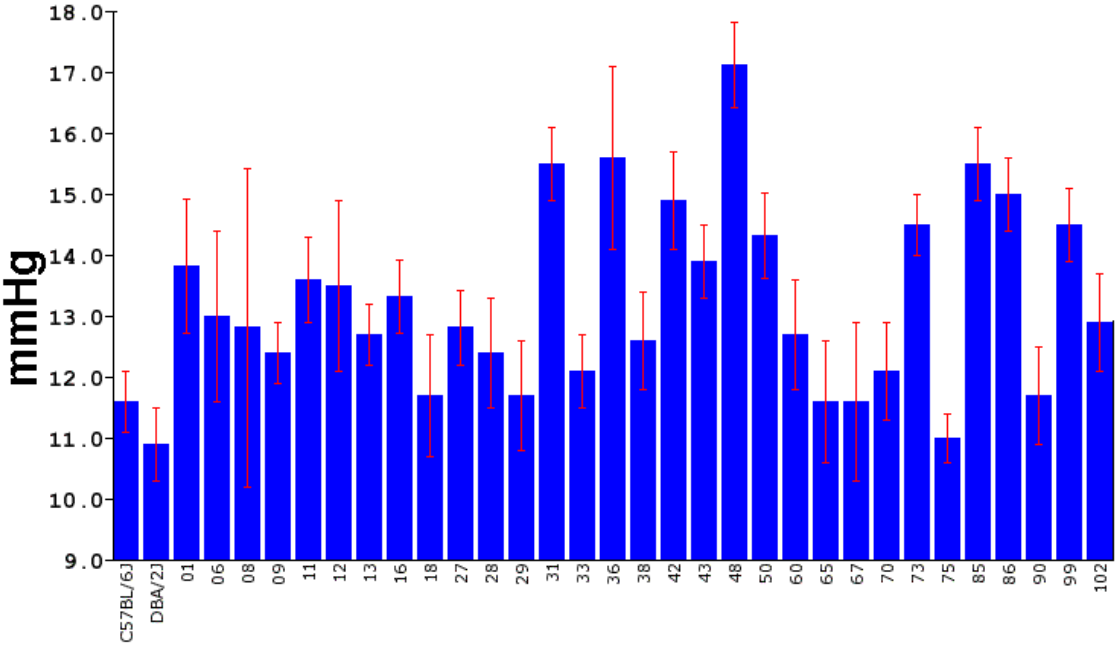

Figure 1. The distribution of IOP measurements across the BXD strains is illustrated in a bar chart with means and Standard Deviations. In the 33 strains of mice the IOP ranged from a low of 10.9 mmHg to a high of 17.1 mmHg.

bioRxiv preprint doi: https://doi.org/10.1101/202937; this version posted October 30, 2017. The copyright holder for this preprint (which was not certified by peer review) is the author/funder. All rights reserved. No reuse allowed without permission.

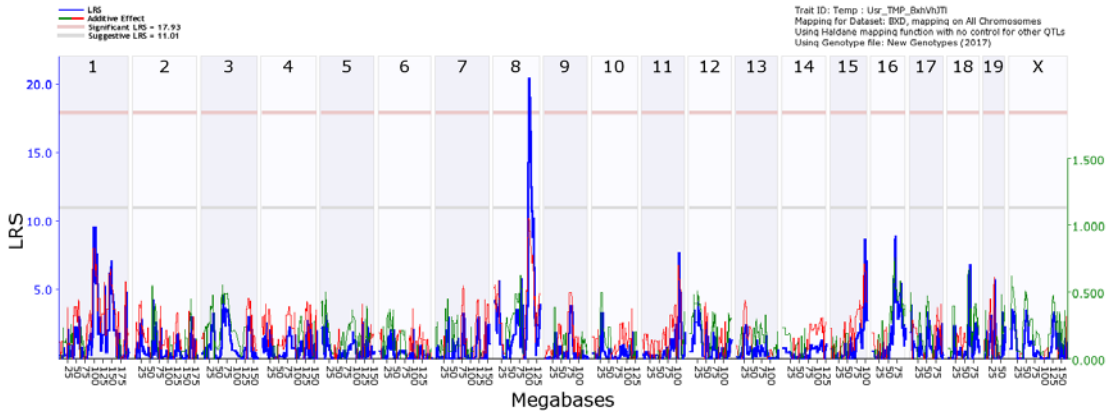

Figure 2. A genome-wide interval map of IOP. The interval map plots the linkage related score (LRS) across the genome from chromosome 1 to chromosome X. The light gray line is the suggestive level and the light red line is genome-wide significance (p = 0.05). When the IOP measures were mapped to the mouse genome there was a significant association between IOP and a locus on Chromosome 8.

bioRxiv preprint doi: https://doi.org/10.1101/202937; this version posted October 30, 2017. The copyright holder for this preprint (which was not certified by peer review) is the author/funder. All rights reserved. No reuse allowed without permission.

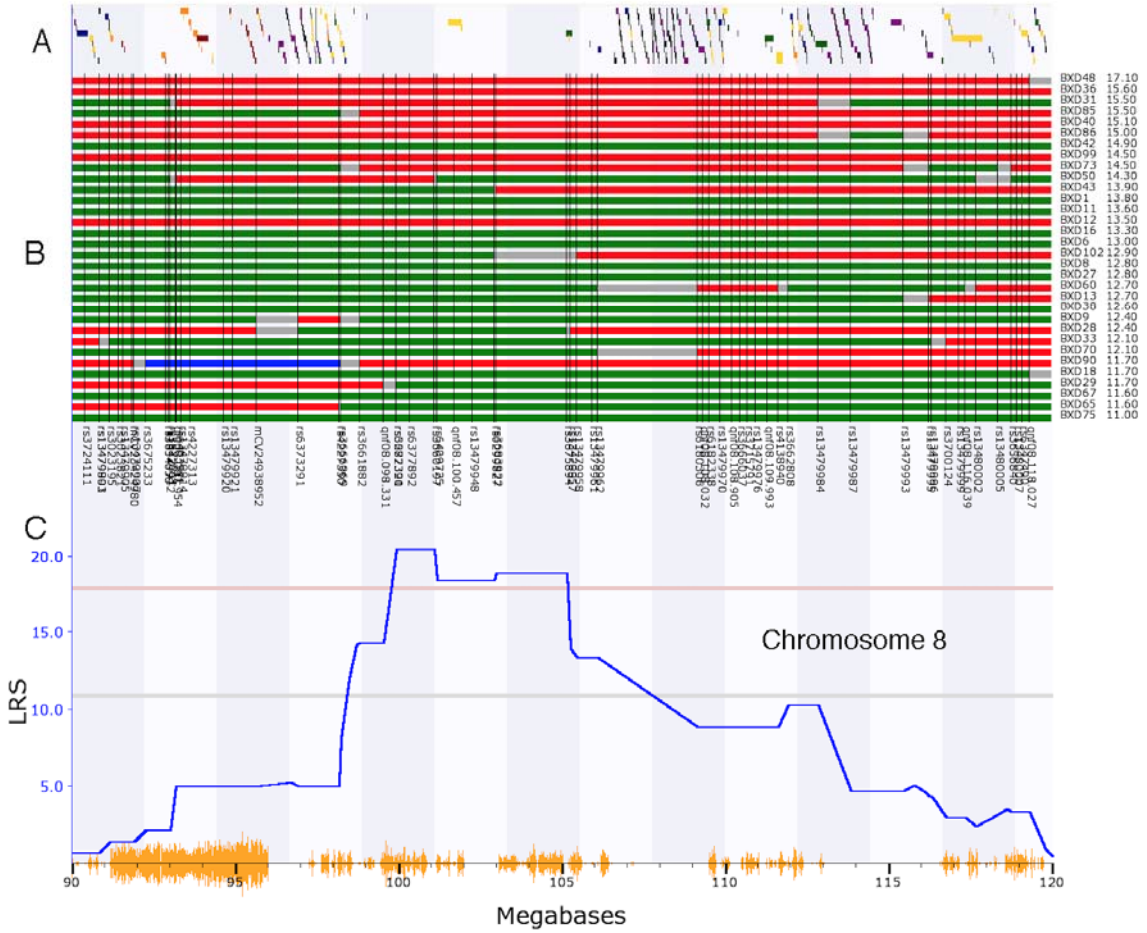

Figure 3. The interval map for Chr. 8: 90 to 120Mb is illustrated. A is the gene tract, that identifies the locations of known genes across the genome. B is a haplotype map for the different BXD RI strains listed to the right and ranked from the highest IOP to the lowest IOP. The location of genomic markers is indicated by black vertical lines. C is an expanded version of the interval map for IOP. Finally, the bottom trace (yellow) identified the location of SNPs between the C57BL/6 mouse and the DBA2/J mouse. The genomic location is indicated along this lower trace. Notice that the peak of the QTL in C sits in a region of the genome that contains very few known genes (A).

bioRxiv preprint doi: https://doi.org/10.1101/202937; this version posted October 30, 2017. The copyright holder for this preprint (which was not certified by peer review) is the author/funder. All rights reserved. No reuse allowed without permission.

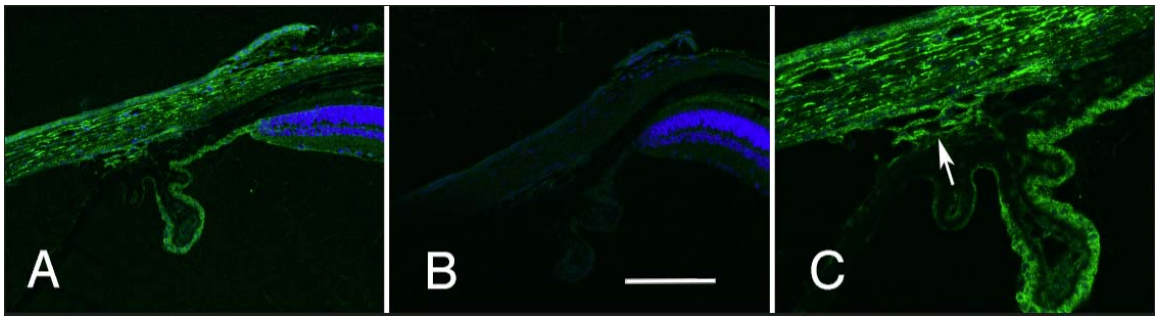

Figure 4. The distribution of cadherin 11 in the limbal area of the eye is illustrated. The section in A was stained with an antibody specific to cadherin 11 (green) and for DNA (blue). This staining is specific to the primary antibody for it is not observed in a section stained with the secondary antibody alone (B). The staining pattern of the trabecular meshwork is shown at higher magnification in C (arrow). A and B are taken at the same magnification and the scale bar in panel B represents 25 µm.

Table 1. Primers designed for Cdh11 and Cdh8 and Myoc

Cdh11	Forward 5’ GAAACCAAAGTCCCAGTGGCC 3’
	Reverse 5’ TGGTCCATTGGCTGTGTCGT 3’
Cdh8	Forward 5’ AGCCTCCGGTCTTCTCTTCAC 3’
	Reverse 5’ CAGTGTGGCGGTCAATGGAAA 3’
Myoc	Forward 5’ GCTGGCTACCACGGACACTT 3’
	Reverse 5’ CGCTCAAGTTCCAGGTTCGC 3’
Ppia	Mm_Ppia_1_SG QuantiTect Primer Assay

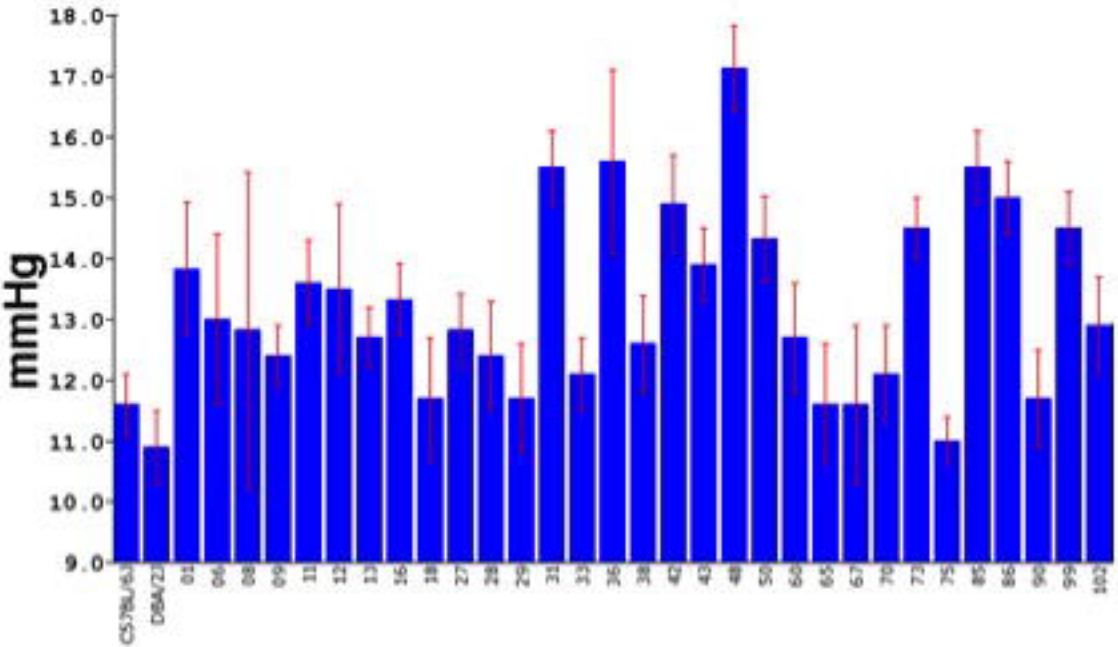
mmHg
18.0
17.0
16.0
15.0
14.0
13.0
12.0
11.0
10.0
9.0
C57BL/6J
DBA/2J
01
06
08
09
11
12
13
16
18
27
28
29
31
33
36
38
42
43
48
50
60
65
67
70
73
75
85
86
90
99
102

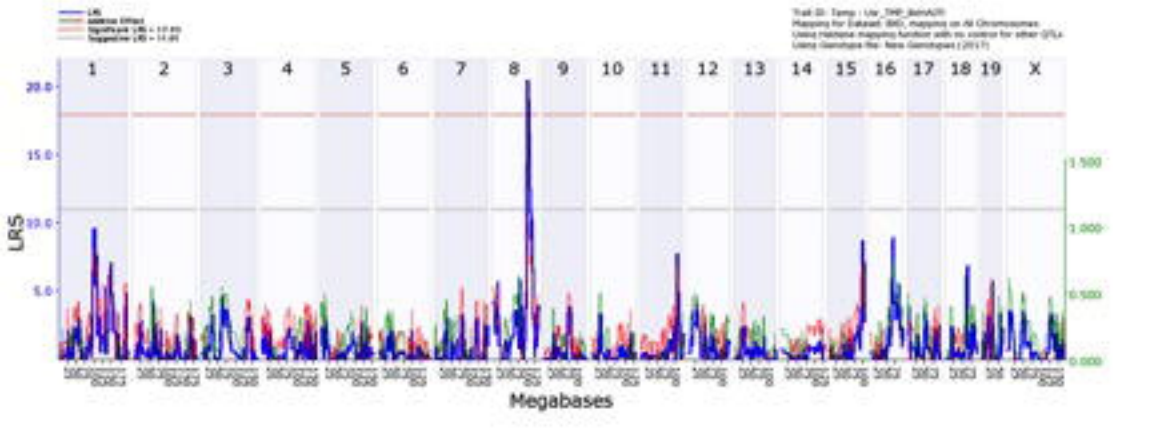
1
2
3
4
5
6
7
8
9
10
11
12
13
14
15
16
17
18
19
X
20.0
15.0
10.0
5.0
LRS
1.500
1.000
0.500
0.000
Megabases

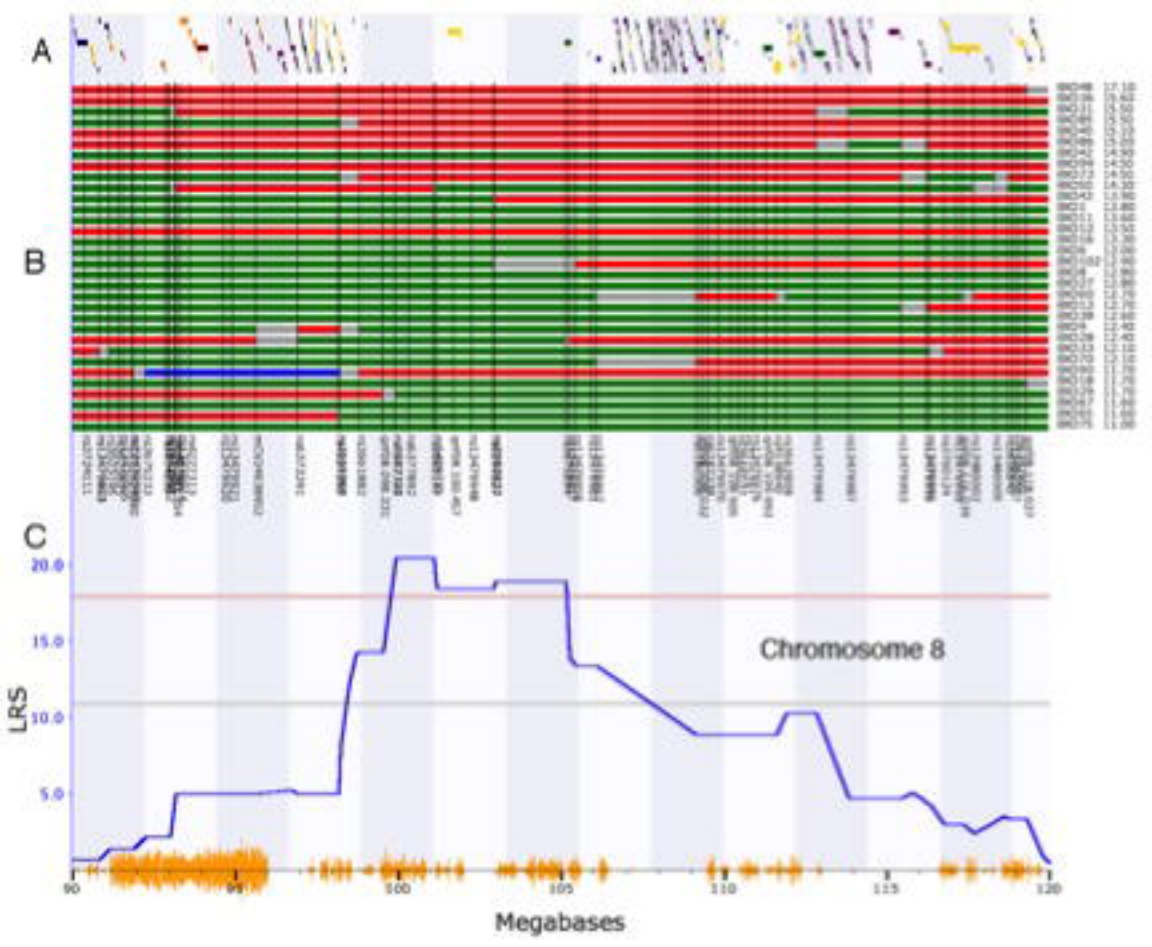
A
B
C
20.0
15.0
10.0
5.0
LRS
Chromosome 8
90
95
100
105
110
115
120
Megabases

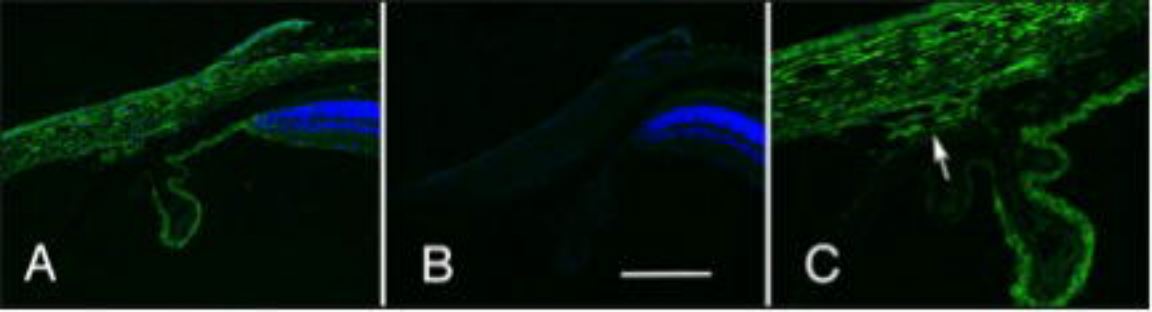
A
B
C